



Matching induction motors to PVG for maximum power transfer

Mehmet Akbaba

*Department of Electrical and Electronics Engineering, University of Bahrain,
P.O. Box 33547, Isa Town, Kingdom of Bahrain
Fax +973-684844; email: akbaba@eng.uob.bh*

Abstract

The matching of 3-phase induction motor to photovoltaic generators (PVGs) for maximum power transfer using enhanced version of Akbaba model for $I-V$ characteristic of PVGs is investigated. Investigations are performed in time domain in order to be able to predict both the transient and as well as steady state performance of the system. The load is a water pump and a double step-up DC to DC converter and a six step voltage source inverter is used as power conditioning unit between the motor and PVG. The power conditioning unit forces the PVG is operated on its maximum power trajectory and power transfer from PVG to water pumping unit, which is composed of motor and pump. The PVG is modeled by recently developed Akbaba model. The system under investigation is fully modeled and the effectiveness and accuracy of the proposed system is demonstrated through numerical results. It is shown that almost full available power of the PVG is utilized and hence maximum power transfer to the motor is achieved. Energy utilization efficiency of as high as 98.3% is achieved.

Keywords: PVG; Maximum power; Water pumping

1. Introduction

Solar energy is one of the most important elements of renewable energy sources and the photovoltaic generators (PVGs) are standing at its heart. It is expected that photovoltaic (PV) power generation will play a key role in meeting future demands for electricity. Therefore the use of PV energy is increasingly being promoted by

governmental policies. For example Japanese government has set an ambitious target of 4.5 GW of electricity to be generated by PV system by the year 2010 [1]. One of the important characteristics of the solar energy is its invariant nature. It does not extract any material from the earth and it does not return any pollutant to the environment. Another important advantage of PV cells is that the main raw material, silicon, is

The Ninth Arab International Conference on Solar Energy (AICSE-9), Kingdom of Bahrain

the second plentiful element available on the earth.

Intensive efforts are being made for developing new processes for manufacturing photovoltaic cells (PVs) and methods for enhancing their conversion efficiency are currently being explored. These efforts aim at reducing the cost per peak watt and narrowing the gap between prices of PVG power and conventional power sources for many applications, such as water pumping systems, especially in isolated areas. It is not economically viable to connect remote areas to the national grid; so water-pumping systems based on PV energy sources are suitable for those areas. In most cases PV water pumping schemes are driven by d.c. motors. Therefore, many studies have been devoted for analysis of cell generator driven d.c. motors [2–10]. Other references are also given in [9,10].

However d.c. motors are most complicated and expensive motors. Sliding brush contacts and commutator are the cause continuous problem and need routine inspection and periodic maintenance. Commutator arcing problem limits the motor size and speed and also makes these motors unsuitable for hazardous areas. Hence the water pumping system based on induction motors, that are more rugged and cheaper than d.c. motors, is a more attractive alternative to the d.c. motor driven PV pumping system. Such a system is more reliable and maintenance-free as compared to d.c. driven system. The only disadvantage of the induction motor based PV pumping system is the increased cost of more complex control circuit. But continuous decrease in the cost of solid state switching devices and rapid increase in their performance/cost ratio overshadows the disadvantage of induction motor-based PV pumping system. On the other hand few investigations devoted to induction motor based PV pumping [11–13]. Therefore in this paper a PV water pumping system driven by a three-phase induction motor is studied. Also some investigations

are repeated to PV water pumping systems based on brushless d.c. motors [14–16]. Since the control of brushless d.c. motors is more complicated than control of induction motor and brushless motors are more expensive it is obvious the PV water pumping systems based on induction motors is more attractive than the ones based on brushless d.c. motors.

Therefore in this paper induction motor-based PV pumping system is considered. The system under investigation is composed of induction motor driven pump load supplied from a PVG via a dc–dc step-up dc–dc converter and a six-step voltage source dc–ac inverter. The whole system is modeled in time domain. Through numerical experiments it is shown that the system under investigation is capable of utilizing the maximum available power of PVG.

2. Modelling the system under investigation

The power source of the pumping system is a PVG. As it is well known that its I – V or V – I characteristic is highly nonlinear. When neglecting the internal shunt resistance, the I – V characteristic of PVGs is given by the following traditional Eqs. (2–7).

$$I = I_{ph} - I_0 [\exp(\Lambda(V + I R_s)) - 1] \quad (1)$$

or as

$$V = -I R_s + (1/\Lambda) \ln[(I_{ph} - I + I_0)/I_0] \quad (2)$$

Eq. (2) is valid for a single cell as well as for cell generators where only the numerical values of the parameters (R_s , Λ , I_{ph} and I_0) are different. In this paper, the PVG given in [2] is taken as the base for comparison between the traditional model and the enhanced version of the Akbaba model. The parameters of this PVG for 100% solar radiation (Maximum solar radiation is taken as 1000 W m^{-2}) are $I_0 = 0.0081 \text{ A}$, $\Lambda = 0.042 \text{ V}^{-1}$, $R_s = 0.90 \text{ } \Omega$, and $I_{ph} = 13.615 \text{ A}$.

Both of the traditional models given in Eqs. (1) and (2) do not easily lend themselves for analytical manipulations. For example, evaluation of the maximum power trajectory requires lengthy iterative process. Also it is not possible to obtain closed form solution for the performance when operating on load. To avoid these difficulties Akbaba [17] has proposed the following model for the I – V characteristic of PVGs

$$I = (V_{oc} - V)/(A + B V^2 - C V) \quad (3)$$

where the coefficient A is the ratio of the open-circuit voltage, V_{oc} , to the, short-circuit current, I_{sc} of the panel, i.e.

$$A = V_{oc}/I_{sc} \quad (4)$$

Power of the PVG then expressed as

$$P = VI = V (V_{oc} - V)/(A + B V^2 - C V) \quad (5)$$

The full details of obtaining parameters A , B , and C are given in ref [17]. Characteristics of the PVG used in this paper is computed for different levels of solar radiation and maximum power trajectory (MPT) are computed from Eqs. (2) and (3) and are compared in Fig. 1. Examination of this Figure shows that the Akbaba model simulates the external I – V characteristics of the solar cell generators very accurately.

The parameters of the Eq. (3) is given directly in percent solar radiation as follows [17]:

$$B = dG^{-e} + fG \quad (6)$$

$$C = gG^{-h} + mG \quad (7)$$

Since parameter A is defined as $A = V_{oc}/I_{sc}$ (Eq. (4)) then V_{oc} and I_{sc} are also expressed in terms of percent solar radiation as follows:

$$V_{oc} = sG^p - qG^2 \quad (8)$$

$$I_{sc} = kG \quad (9)$$

where G is the *percent solar radiation*, the values of the curve fitting coefficients $d, e, f, g, h, k, m, p, q$ and s are obtained as [20]: $d = 0.015, e = 1.095, f = 0.00000021, g = 7.5, h = 0.99, m = 0.000045, s = 82.4108, p = 0.173, q = 0.00064, k = 0.13608$.

To examine the accuracy of this new model, the model parameters A, B , and C are computed using the original PVG data in the original diode model equations, Eqs. (1) and (2), as described in Akbaba and Alattawi [19]. Subsequently they are compared with the Eqs. (6)–(10) in [17] and it is clearly shown that all parameters of the model are expressed in terms of solar radiation level very accurately. Therefore with this enhancement, the performance of PVG can be evaluated in closed form, using only one single input data, which is the percent solar radiation G , besides the external equations that would govern the load behavior.

Due to high initial cost of the PV panels, it is imperative to operate the panels, as much as possible, close to their maximum power trajectory. Therefore, our interest is to obtain maximum power point voltage and current. With the traditional model, time consuming and boring iterative solutions are inevitable. Moreover, this process is required for each solar radiation level. In the following, a closed form solution is provided for this problem.

Maximizing Eq. (5) with respect to the voltage gives the following equation for maximum power point voltage V_{max} [17]:

$$V_{max} = [V_{oc} / (I_{sc} (C - B V_{oc}))] \cdot [1 - (1 - I_{sc} (C - B V_{oc}))^{0.5}] \quad (10)$$

Having obtained maximum power point voltage from Eq. (10), then maximum power point current and maximum power can be computed directly from Eqs. (3) and (5) respectively.

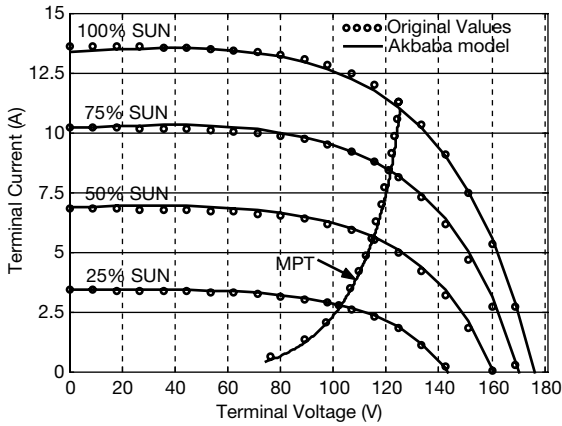


Fig. 1. Comparison of $I-V$ characteristics and MPT between original values and Akbaba Model. MPT: maximum power point trajectory.

Hence the original $I-V$ characteristics and maximum power trajectory (MPT) obtained from traditional model given by Eq. (2) are compared with their counterparts obtained from Akbaba model [17] (Eqs. (3) and (5)) are included in Fig. 1. The accuracy of the proposed method is clearly noted from this figure.

The system under investigation is composed of an induction motor driven water pump as load that is supplied from a PVG, via a double step-up d.c.–d.c. converter and a six-step voltage source d.c.–a.c. inverter (VSI). The block diagram of the complete PV pumping system under investigation is given in Fig. 2 and circuit diagram of the double step-up d.c.–d.c.

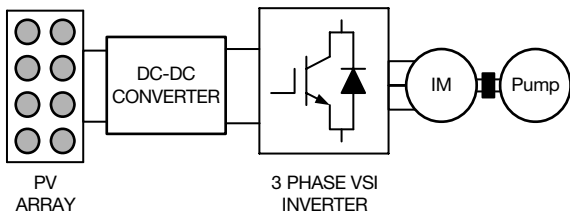


Fig. 2. Block diagram of the PV pumping system under investigation.

converter is given in Fig. 3. The circuit diagram of a VSI, its operating principles and modeling can be obtained in many power electronics textbooks [18].

Modeling of the double step-up d.c. to d.c. converter is given in [17] in full details and will not be repeated here.

The induction motor is modeled in synchronously rotating reference frame as given in Eq. (11) and the water pump is modeled as given Eq. (14) in the following text.

$$\begin{bmatrix} v_{qs} \\ v_{ds} \\ v'_{qr} \\ v'_{dr} \end{bmatrix} = \begin{bmatrix} R_s + pL_s & \omega L_s & pL_m & \omega L_m \\ -\omega L_s & R_s + pL_s & -\omega L_m & pL_m \\ pL_m & \omega_{sl}L_m & R'_r + pL'_r & \omega_{sl}L'_r \\ -\omega_{sl}L_m & pL_m & -\omega_{sl}L'_r & R'_r + pL'_r \end{bmatrix} \begin{bmatrix} i_{qs} \\ i_{ds} \\ i'_{qr} \\ i'_{dr} \end{bmatrix} \quad (11)$$

where p is the differential operator (d/dt), and

$$L_m = \frac{3}{2}L_{ms}, \quad L_s = L_{\sigma s} + L_m \quad \text{and} \quad L'_r = L'_{\sigma r} + L_m$$

and ω_{sl} is the slip speed and it is computed from the following equation:

$$\frac{d\omega_{sl}}{dt} = -(P_o/J)(T_e - T_p) \quad (12)$$

where T_e is the electromagnetic torque and T_p is the water pump torque. The electromagnetic torque of the machine can be written as

$$T_e = (3/2) P_o L_m (i_{qs} i'_{dr} - i_{ds} i'_{qr}) \quad (13)$$

and T_p is given as

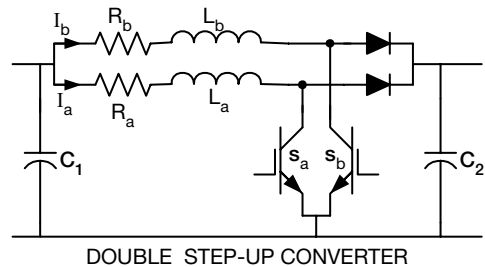


Fig. 3. Circuit diagram of double step-up d.c. to d.c. converter.

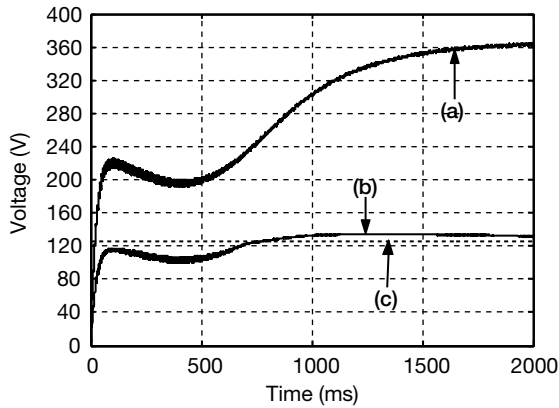


Fig. 4. Variation of the PVG output voltage and double step-up d.c. to d.c. converter output voltage vs. time: (a) PVG output voltage; (b) d.c. to d.c. converter output voltage versus time; (c) maximum power point voltage (V_{\max}).

$$T_p = k_{p1}(\omega - \omega_{sl}) + k_{p2}(\omega - \omega_{sl})^2 \quad (14)$$

where ω is the speed of rotating reference frame and synchronously rotating reference frame is used. The pump torque constants are given as $k_{p1} = 0.0000023 \text{ Nm/rad/s}$ and $k_{p2} = 0.0055 \text{ Nm/(rad/s)}^2$. Parameters of the induction motor and double step-up converter are given in Appendix A and meanings of various symbols are given in the nomenclature.

3. Results and discussions

To the steady state and transient performance of the system under investigation Eqs. (3)–(14) are programmed in MATLAB computing environment. Results are obtained for 100% solar radiation, which is taken as 1000 W/m^2 , and demonstrated in Figs. 4–6.

Fig. 4 shows the variation of the PVG out voltage vs. time and double step-up d.c. to d.c. converter output vs. time. Also the maximum power point voltage of the PVG, which is 124.8 V for the PVG under investigation, is included in this figure. From this figure we observe the following important results:

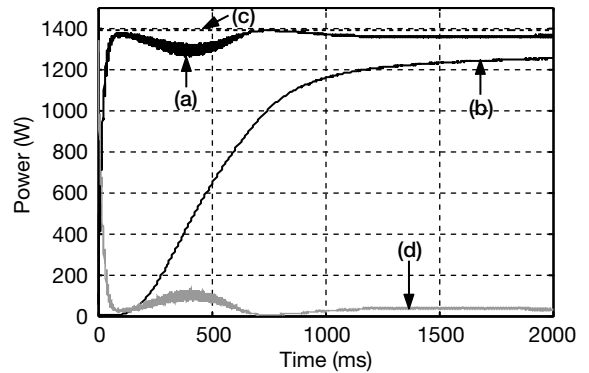


Fig. 5. Variation of various powers vs. time; (a) PVG output power; (b) Motor output power; (c) Maximum available power of PVG; (d) Mismatch power.

– The output voltage of the PVG approached the maximum power point voltage, which is a clear indication of the fact that at steady state, the PVG operates almost on its maximum power trajectory and nearly full available energy of the PVG is utilized. A further proof of this will be given through observation of the Fig. 5 that is given below.

– The output voltage of the double step-up d.c. to d.c. converter is stepped up in a level that just suitable for the motor, for maximum power utilization. This indicated that step-up converted is operating as a maximum power point tracker (MPPT). But in order the double step-up converter, which is a voltage step-up chopper, to operate as MPPT a correct value must be used for the duty cycle of the chopper switches S_a and S_b . Through the numerical experiments it was observed that most favorable chopper duty cycle is 0.46 (46%) for the system under investigation. This value of the chopper duty cycle is valid for all levels of solar radiation.

Fig. 5 depicts the variation of the PVG output power, motor output power, maximum available power of PVG, i.e., the maximum power that PVG can deliver if there is 100% perfect matching between the PVG and the load, and mismatch power vs. time. Mismatch power

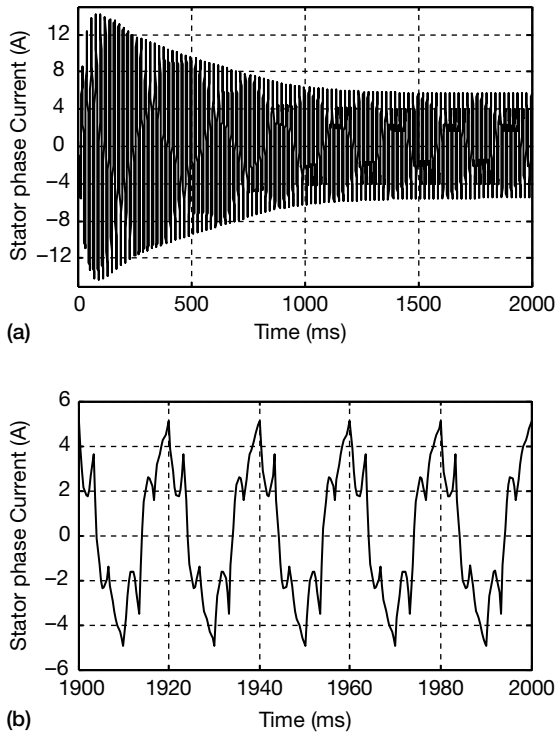


Fig. 6. Transient and steady-state motor phase currents vs. time; (a) transient current; (b) steady-state current.

is defined as difference between the maximum available power of PVG (P_{\max}) and actual operating output power of PVG when it is connected to the load. It is obvious from this figure that at steady-state operation PVG operates almost on its maximum power trajectory. The mismatch power is not more than a few W at steady state operation. The motor output power reaches to 1256 W, which is less than PVG power by the losses of the motor and power conditioning circuitry between the PVG and motor.

The above results clearly show that the PV water-pumping scheme proposed in this work is utilizes the PVG power very efficiently. Energy utilization efficiency, which is defined as the ratio of PVG output power to P_{\max} , is very high. At steady-state PVG output power is 1368 W, where as $P_{\max} = 1392$ W. Therefore energy utilization efficiency is $1368/1392 = 98.3\%$, which

is near to perfect. The mismatch power is only 1.7%. The operating efficiency at steady state is $1256/1368 = 91.8\%$. Hence the proposed PV water pumping system shows promising future. Further minimization of the energy losses due to motor itself is possible by using energy efficient cage induction motors instead of standard efficiency motors. The energy efficient induction motors are at least 3% more efficient than standard efficiency motors. Therefore with use of energy efficient motors the operating efficiency could be improved up to 95%. Although energy efficient motors are a little more expensive than standard efficiency motors, but the cost of saved energy can cover the price difference within a few years in case of retrofit and within few months in case of a new installation [20].

Finally the transient and steady state motor phase currents are depicted in Fig. 6. Although this figure do not yield any result regarding the efficiency of the matching process, but it is a good indication of the correct modeling of the whole system, as it gives the expected wave-shape when an induction motor is supplied from a six step VSI. It warts mentioning here that the transient time duration with PVG power source is much longer as compared to the case. When the inverter input is a constant d.c. power source. But for a water pumping drive this drawback is not important.

4. Conclusions

This paper focuses on the matching of a 3-phase induction motor driven water-pumping system to PV array for maximum energy transfer. The system is composed of a PV array, a d.c. to d.c. step-up converter working as an MPPT, an induction motor and a centrifugal water pump. In order to investigate both the transient and the steady-state performance, the whole system is modeled in time domain. The PV array is modeled using Akbaba model, which introduces a great computational simplification.

It is found that with proper choice of a value for the duty cycle of the step-up converter, the PV array operates almost at its maximum power trajectory and maximum energy is transferred to the motor-pump combination. The mismatch power, which is defined as the difference between the maximum available power of PV array (P_{\max}) and its actual operating output power, is not more than a few watts (about 1.7%), resulting in an energy utilization efficiency of 98.3%. The operating efficiency of the system was found to 91.8%, and it is recommended that the operating efficiency could be improved further by using energy efficient motors. At power levels of the PV water pumping system, the energy efficient induction motors are at least 3% more efficient than standard efficiency motors. Therefore with use of energy efficient motors the operating efficiency could be improved up to 95%. Considering the robust, maintenance free and low cost characteristics of 3-phase induction motors, it is evident that induction motor based PV water pumping systems will become very popular in the near future.

Nomenclature

C_1 and C_2	PVG terminal and DC link voltage filter capacitors respectively
I_{ph}	light generated current (photocurrent)
I_o	reverse saturation current
J	inertia of the pump motor–pump combination
L_a and L_b	inductances of the chopper inductors respectively
L_m	magnetizing inductance between stator and rotor windings
L_{ms}	magnetizing inductance of the stator windings
L_s and L'_r	stator and rotor winding self inductances in d-q frame (referred to stator side)

L_{os} and L'_{or}	stator and rotor leakage reactances respectively (referred to stator side)
P_o	number of pole pairs
R_a and R_b	resistance of the chopper inductors respectively
R_s	series resistance of the PVG
R_s and R_r	stator and rotor resistances respectively (referred to stator side)
S_a and S_b	controlled semiconductor switches for double step step-up d.c. to d.c. converter
Λ	PVG constant (V^{-1})

References

- [1] H. Asano, K. Yajima and Y. Kaya, Influence of photovoltaic power generation on required capacity for load frequency control, *IEEE Trans. Energy Convers.*, 11 (1996) 188–193.
- [2] J. Appelbaum, Starting and steady-state characteristics of DC motors powered by solar cell generators, *IEEE Trans. Energy Convers.*, 1 (1986) 17–25.
- [3] P.K. Koner and J.C. Joshi, Matching analysis of photovoltaic powered dc derives motors and centrifugal pumps by varying motor constants *Int. J. Energy. Res.*, 16 (1992) 301–313.
- [4] M.M. Saied, Matching of DC motors to photovoltaic generators for maximum daily gross mechanical energy, *IEEE Trans. Energy Convers.*, 3 (1988) 465–472.
- [5] M.M. Saied and A.A. Hafnafy, Optimal design parameters for a PV array coupled to a DC motor via a DC-DC transformer, *IEEE Trans. Energy Convers.*, 4 (1991) 593–598.
- [6] S.M. Alghuwainern, Steady-state performance of DC motors supplied from photovoltaic generators with a step up converter, *IEEE Trans. Energy Convers.*, 7 (1992) 267–272.
- [7] H. Hilmer, A. Ratka, K. Vajen, H. Ackermann, W. Fuhs and O. Melsheiner, Investigation of directly coupled photovoltaic pumping system connected to a large absorber filed, *Sol. Energy*, 61 (1997) 65–76.
- [8] M. Akbaba, I. Qamber and A. Kamal, Matching of separately excited dc motors to photovoltaic

- generators for maximum power output, *Sol. Energy* 63 (1998) 375–385.
- [9] M. Akbaba and M.C. Akbaba, Dynamic analysis of a photovoltaic-boost converter powered dc motor pump system, In proceedings of IMDC-IEEE conference, Boston, USA, 2 (2001) 356–361.
- [10] M.M. Saied, The available matching of solar arrays to the dc motors having both constant and series excited field components, *IEEE Trans. Energy Convers.*, 3 (2002) 301–305.
- [11] S.R. Bhat, A. Pittet and B.S. Sonde, Performance optimization of induction motor-pump system using photovoltaic energy source, *IEEE Trans. Ind. Appl.*, IA-23 (1987) 995–1000.
- [12] M.Z. Aziza and M.N. Eskander, Matching of Photovoltaic motor-pump systems for maximum efficiency operation, *Renewable Energy*, 7(3) (1996) 279–288.
- [13] M.N. Eskander and M.Z. Aziza, A Maximum Efficiency-Photovoltaic-Induction motor pump system, *Renewable Energy*, 10(1) (1997) 53–60.
- [14] D. Langridge, W. Lawrance and B. Wichert, Development of a photovoltaic pumping system using a brushless d.c. motor and helical rotor pump, *Sol. Energy*, 56 (1996) 151–160.
- [15] C.L.P. Swamy, B. Singh and B.P. Singh, Dynamic performance of a permanent magnet brushless DC motor powered by a PV array for water pumping, *Sol. Energy Mater. Sol. Cells*, 36 (1995) 187–200.
- [16] C.L.P. Swamy, B. Singh, B.P. Singh and S.S. Murthy, Experimental investigations on a permanent magnet brushless DC motor fed by a PV array for water pumping system, *J. Sol. Energy Eng. T. ASME*, 122 (2000) 129–132.
- [17] M. Akbaba, Matching 3-phase ac loads to PVG for maximum power transfer using enhanced version of Akbaba model and double step-up converter, *Sol. Energy*, 75(1) (2003) 17–25.
- [18] M.H. Rashid, *Power Electronics*, 2nd edn, Prentice Hall, New Jersey, 1993, 364–372.
- [19] M. Akbaba and M.A.A. Alattawi, A new model for I–V characteristic of solar cell generators and its applications, *Sol. Energy Mater. Sol. Cells*, 37 (1995) 123–132.
- [20] M. Akbaba, Energy conservation by using energy efficient electric motors, *Appl. Energy*, 64(1) (1999) 149–158.

Appendix A

Parameters of the induction motor used:

$$R_s = 2.132 \, \Omega, R_r = 2.096 \, \Omega, L'_{gs} = 14.089 \, \text{mH}, \\ L'_{gr} = 14.089 \, \text{mH}, L_m = 942.67 \, \text{mH}, \\ 260 \, \text{V}, 50 \, \text{Hz}, 4 \, \text{pole}, J = 0.0224 \, \text{kg m}^{-2}.$$

Parameters of the double step-up converter:

$$L_a = L_b = 1.2 \, \text{mH}, R_a = R_b = 14 \, \text{m}\Omega; C_1 = C_2 = 450 \, \mu\text{F}, \\ \text{Chopper frequency} = 5 \, \text{kHz}.$$